3.5 GHz WiMAX GaN Doherty Power Amplifier with 2nd harmonic tuning

3.5 GHz WiMAX GaN Doherty Power Amplifier with 2nd harmonic tuning

Jie Fang, Jorge Moreno, Roberto Quaglia, Vittorio Camarchia, Marco Pirola, Simona Donati Guerrieri, Chiara Ramella, Giovanni Ghione

Department of Electronics and Communications (DET), Politecnico di Torino, Corso Duca degli Abruzzi, 24, 10129 Torino, Italy.

Abstract

The paper presents the design, realization, and experimental validation of a GaN-based hybrid Doherty power amplifier for WiMAX base-stations at 3.5 GHz. The amplifier exploits, for the first time as far as authors' knowledge goes, a second harmonic tuning scheme designed to further improve the efficiency in the Doherty region. The amplifier is based on a packaged GaN HEMT from Cree Inc., and shows a saturated output power exceeding 43.2 dBm (21.5W), a Doherty high efficiency region in excess of 6 dB output back-off, with a first peak and maximum drain efficiency at saturation of 55% and 61%, respectively. The amplifier, with baseband digital predistortion, is compliant with the standard emission mask in presence of a 9 dB PAPR WiMAX input, and exhibits a weighted efficiency as high as 40%. The performances of the designed amplifier favorably compare with the state of the art for the same application.

Doherty power amplifiers, high efficiency amplifiers, GaN-based FETs, WiMax, PA linearization

Corresponding author

Vittorio Camarchia

Dep. of Electronics - Politecnico di Torino

C.so Duca degli Abruzzi 24

I-10129 Torino, Italy

tel. +39-011-0904219

fax +39-011-0904099

email vittorio.camarchia@polito.it

I INTRODUCTION

Last generation wireless communication standards are conceived to satisfy the continuously increasing demand of high data rate services. This request can be satisfied through strategies providing high spectral efficiency [1],[2], e.g. Code Division Multiple Access (CDMA), or Orthogonal Frequency Division Multiplexing (OFDM), adopted in UMTS and WiMAX communication standards, respectively. From the standpoint of Power Amplifier (PA) design, the high dynamics of the base-band modulating signals require a different approach to the paradigm of PA efficiency. In fact, the well-established high efficiency PA design strategies for constant envelope signals are not suited for modulations with Peak to Average Power Ratio (PAPR) of several dBs. In this context, the Doherty scheme [3] represents a favorable PA architecture to deal with non-constant envelope signals, since it maintains high efficiency levels on a wide range of output powers [4]-[6].

Doherty PAs based on LDMOS technology have been already adopted for frequencies around 2 GHz [7],[8], but higher frequency applications require more advanced technologies. Among these, the one based on GaN devices (already actively investigated and exploited for RF and microwave power applications up to the X-band) seems to be well suited also for 3G wireless systems. Despite this, only a few results above the 2.14GHz WiFi band have been published so far on GaN technology [9]-[13].

From the design standpoint, the 2nd harmonic tuning approach [14-[15]] is a well-established technique for high efficiency single stage power module but, as far as the authors' knowledge goes, has not yet been successfully applied to a Doherty stage, mainly because this approach requires the needed phase and modulus relationships between fundamental and 2nd harmonic components to be maintained across the whole high efficiency Doherty region.

In the present paper, the design and linearization of a 2nd harmonic tuned Doherty PA for WiMAX applications at 3.5 GHz based on Cree Inc. GaN devices, with enhanced performances with respect to its prototype version [16], are presented and discussed.

Continuous Wave (CW) characterization has shown a maximum output power of 21.5 W, with maximum efficiency of 61 %, and efficiency at 6 dB and 9 dB Output Back-Off (OBO) of 55 % and 40 %, respectively. Concerning the PA linearity, a base-band digital predistortion scheme based on a Parallel Hammerstein approach [17] has been designed and tested. The linearized amplifier, complying with the highest dynamic WiMAX signals, operates at an average output power of 34.2 dBm (2.8 W), i.e. roughly 9 dB below the maximum output power. The average efficiency is around 40 %, with a gain of the linearized PA of 10 dB.

The realized Doherty power module performances favorably compare with the most relevant papers on GaN for this specific application (see Table 1).

Table 1 Comparison between the designed PA and some of the most relevant papers published on GaN WiMAX amplifiers

Reference	$P_{OUT,MAX}$ (W|dBm)	η_{MAX} (%)	$\eta_{6\,dB}$ (%)	η_{9dB} (%)	GaN Device
2007[11]	160|52	51	34	27.8	Eudyna-90W
2008[12]	18|42.5	57	48	40	Cree-10W
2010[13]	32|45	67	42.7	32	RFHIC-16W
This Work	**21.5|43.2**	**61**	**55**	**40**	**Cree-10W**

The paper is organized as follows: Section II presents the amplifier design strategy, highlighting the key aspects considered. Section III describes the CW characterization results. The baseband digital predistortion scheme and its implementation are described in Section IV, where the linearization results are also presented and commented. Finally, some conclusions are drawn in Section V.

II DESIGN STRATEGY

GaN FET devices grown on SiC substrates represent at present a promising solution for the development of RF PAs. In fact, thanks to GaN favorable electrical behavior in terms of current density, breakdown voltage, and cut-off frequency, and to the remarkable thermal characteristics of the SiC substrate [18],[19], GaN based power modules handling tens of Watts, up to the X-band and beyond, can be realized. In this framework, we present a high efficiency 21.5 W Doherty PA designed for WiMAX at 3.5 GHz. The adopted device is the CGH40010 from Cree inc., a packaged GaN HEMT on SiC with typical 10 W of $P_{OUT,1dB}$ in C-band, at a drain bias of 28 V [20].

As a preliminary design step, an *ad-hoc* characterization campaign has been carried out on the CGH40010 GaN HEMT active device for the identification and deembedding of the device parasitics [21]. The Doherty main stage follows the 2nd harmonic tuning design strategy, while the peak unit implements a class C (see Fig. 1) power module.

FIG 1 HERE

Fig. 1: Block diagram of the designed Doherty amplifier.

In 2nd harmonic tuning, the maximum fundamental drain voltage span is higher than the difference between bias and knee voltages (as in tuned load approach), because the proper addition of the 2nd harmonic to the fundamental component raises the minimum total drain voltage above the knee voltage hence preventing early compression of the fundamental tone. Thanks to the high breakdown voltage of GaN devices, the resulting drain voltage overshoot [14] does not require any DC drain bias reduction, as would be the case of PAs based on traditional devices that need a bias centered between breakdown and knee voltages.

This increase of the voltage swing at fundamental produces, at list in theory, a maximum output power $\sqrt{2}$ times higher than in tuned load, with direct impact on the efficiency.

To correctly apply this strategy the 2nd harmonic load termination has to be optimized (3rd harmonic shorted), and the input driving voltage should be properly shaped to produce fundamental and 2nd harmonic drain voltages with opposite phases.

This concept has been already applied in single stage PAs, where the main goal is to maximize the peak efficiency at a specific output power level, at which the required amplitude and phase relationships between fundamental and second harmonic [22] are implemented. In a Doherty module these relationships must be enforced and maintained across the whole Doherty region, a rather challenging objective that can be reached only through well focused and accurate optimization in the design phase, and precise tweaking during characterization. As far as the authors' knowledge goes this amplifier represents the first successful attempt to extend the second harmonic tuning strategy to a Doherty PA.

Fig. 2, and Fig. 3 report the simulated drain voltage waveforms at the onset of the Doherty region and in saturated conditions, respectively. From these figures it is clear, for the two power levels limiting the Doherty region, that fundamental and 2^{nd} harmonic properly combine in amplitude and phase keeping the total drain voltage always above the knee voltage.

FIG 2 HERE

Fig. 2: Simulated drain voltage waveforms at 6 dB OBO (37.2 dBm): complete waveform (redline), fundamental (blue dotted line), and 2^{nd} harmonic (green dashed line).

FIG 3 HERE

Fig. 3: Simulated drain voltage waveforms at saturated output power (43.2 dBm): complete waveform (red line), fundamental (blue dotted line), and 2^{nd} harmonic (green dashed line).

Fig. 4, depicts in more detail this feature as a function of the output power. In fact, it shows, as a function of the output power, the simulation results on the fundamental and 2^{nd} harmonic amplitude, together with their phase difference, at the main stage output. The obtained behavior can be seen to be in rather good agreement, all across the Doherty region, with the theoretical results provided in [14].

FIG 4 HERE

Fig. 4: Simulated amplitude of the fundamental (blue) and 2nd harmonic (green) of the main amplifier, together with their phase difference (black) versus output power.

According to the 2nd harmonic tuning approach, the main stage optimum load R_{opt}=30 Ω has to be increased by a factor of $\sqrt{2}$. The resulting output matching network, thanks to a λ/4 impedance transformer, synthesizes a load of $2\sqrt{2}\,R_{opt}$ below the Doherty region, and $\sqrt{2}\,R_{opt}$ at saturation, while another λ/4 line has been inserted to match the external 50Ω load.

The peak output matching network has been designed to maximize the drain current and efficiency in the Doherty region controlling the fundamental and 2nd harmonic terminations, and, at the same time, to ensure at low power drive level (i.e. when the peak module is still off), the highest impedance at fundamental seen from the common node with the main amplifier.

Fig. 5 shows the distributed topologies used for the main and peak output matching networks.

FIG 5 HERE

Fig. 5: Output matching network scheme of the Doherty PA.

The input matching network of the main amplifier has been designed to provide an input voltage according to the 2nd harmonic strategy. To achieve the 2nd harmonic complete phase inversion of the drain voltage, the additional delay introduced by a complex load at the 2nd harmonic drain termination has been exploited [14].

Broad-band unconditional stability of main and peak GaN FETs has been enforced inserting RC networks on the input matching networks of both stages.

III PA CW CHARACTERIZATION

The Doherty amplifier has been fabricated on a Taconic substrate with copper metallization (RF35 with ε_r=3.5, height of the substrate H=0.76 mm, and metal thickness t=0.035 μm), and mounted on a brass carrier, see Fig. 6.

FIG 6 HERE

Fig. 6: Picture of the realized Doherty PA.

The PA has been characterized in DC, small-signal, and CW single tone excitation at 3.5GHz [23],[24], with nominal bias $V_{DS,main}$=28 V, $V_{GS,main}$=-2.73 V (10% I_{DSS}), $V_{DS,peak}$=28 V, and $V_{GS,peak}$=-7 V. Bias tuning has been carried out (see [25]) to optimize the amplifier performances.

The DC currents of the two stages have been separately measured to evaluate the correct *switching on* of the peak amplifier at the onset of the Doherty region. The resulting behavior is well in agreement with the expected trend, as highlighted in Fig.7.

Fig.8 shows the good agreement between simulated and measured S_{11} and S_{21} of the Doherty amplifier at the optimized bias point. The input reflection coefficient S_{11} resulted to be lower than -10 dB over a 170 MHz bandwidth.

FIG 7 HERE

Fig.7: Main (red), and peak (blue) DC drain currents versus output power. Lines refer to simulations, while symbols to measurements.

FIG 8 HERE

Fig.8: Comparison of the Doherty amplifier S_{11} (red), and S_{21} (blue). Lines refer to simulations, while symbols to measurements.

The simulated and measured drain efficiency and gain of the Doherty amplifier as a function of the output power are shown in Fig. 9.

The agreement between measurements and simulations is good, although the measured efficiency is somewhat lower than the expected one. The two efficiency peaks predicted by the Doherty theory are clearly observable, and the measured drain efficiency is higher than 55 % in a 6 dB OBO, with a remarkably flat behavior.

FIG 9 HERE

Fig. 9: 3.5 GHz, CW Single Tone PA characterization. Power Gain (blue), and Efficiency (red) versus output power. Lines refer to simulations, while symbols to measurements.

IV PA BASE-BAND PREDISTORTION

PAs are affected by AM-AM and AM-PM distortion, caused by nonlinear active device behaviors and thermal memory effects [26]. In Doherty modules, issues more specifically related to its architecture, i.e. slow wake up of the peak amplifier, should also be considered. To increase the PA linearity and to ensure the compliance with the WiMAX standard, we introduce a digital predistorter (DPD). A rather conventional but simple and robust scheme has been chosen, with a view at the practical implementation of the DPD. While in [16] we have shown linearization effectiveness with 5 MHz bandwidth & 6 dB PAPR signals, in this work we consider a more challenging and realistic case, with a system of Type G [27], adopting 7 MHz bandwidth signal with PAPR of 9 dB. The available instrumentation limited the characterization bandwidth to 7 MHz (other WiMAX systems can have bandwidth up to 28 MHz); however, DPD results are

expected to be affected at high bandwidth only to a minor extent, due to the limited memory effects of this stage.

The DPD has been designed through the indirect learning approach [28]: the measured input and output base-band signals are interchanged to identify a postdistorter which then is used as the DPD. Indirect learning is extremely effective in terms of extraction computation time and ease of identification, since it does not require the inverse of a dynamic nonlinear model to be computed. In this case, a baseband PA model is not required for DPD extraction, even if this can be useful to validate the linearization effectiveness of the DPD+PA chain at a software (simulation) level before the actual hardware implementation of the DPD.

FIG 10 HERE

Fig. 10: Scheme of the Memory Polynomial base-band model.

The base-band PA and DPD models are implemented adopting a Memory Polynomial (MP) scheme, a parallel architecture (Fig. 10) whose branches are conceived as Hammerstein non-linear models [17]. Static non-linearities are represented through an odd monomial form of order *p*, while memory is accounted for through a *m* tap FIR filter. A clear advantage of the MP model is that, once conveniently rewritten, it can be interpreted as a linear model, and its coefficients can be directly extracted through linear regression algorithms.

The Doherty base-band behavior has been characterized with the experimental setup shown in Fig. 11: the PA is driven with the Agilent ESG E4433B arbitrary waveform generator, while measurements are collected by the Agilent MXA N9020A vector analyzer controlled by the Agilent vector signal analyzer software. Input and output base-band signals are used to identify both PA and DPD models. The PA bias currents and voltages are acquired for computation of average efficiency under modulated conditions. The same setup has also been used to test the linearized PA behavior, feeding the ESG with the predistorted signal.

FIG 11 HERE

Fig. 11: Setup of the base-band characterization setup.

Concerning the PA model, a twelfth order polynomial (p=12), with memory depth of two (m=2) has been found accurate enough to account for the non-linearities and memory effects. Regarding the DPD, further attention must be paid to the selection of p and m, since minimizing the DPD complexity becomes an added goal, above all in consideration of the DPD FPGA final implementation. In fact, the model complexity directly impacts on computational cost, occupied area, and power consumption of the digital section.

A reasonable trade-off between DPD complexity and linearization effectiveness has been found to be p=8 and m=2, values already demonstrated to be compatible with FPGA implementation [22].

FIG 12 HERE

Fig. 12: Normalized output spectrum of the PA with (red) and without (blue) DPD, together with the WiMAX emission mask (black) [27].

Fig. 12 shows the PA performances with a 9 dB PAPR WiMAX signal: while compliance with the WiMAX emission mask is not verified without predistortion, DPD insertion allows to comply with the specifications of the standard.

The spectra refer to an average output power of 34.2 dBm corresponding to 9 dB back-off with respect to the amplifier maximum power. In these conditions, an average drain efficiency around 40 %, corresponding to a PAE of 36 %, is achieved.

As a final remark, note that the average power at which the predistorter was extracted has been chosen to provide a linearized PA gain (in our case 10 dB) close to the PA gain in CW conditions at the same output power. In other words, this means that our DPD is ensuring optimized performances of the linearized amplifier not reducing the PA gain.

V CONCLUSIONS

A second harmonic tuned Doherty GaN based power amplifier operating at 3.5 GHz for WiMAX applications has been designed, realized and characterized both in CW and under WiMAX modulated signals. From base-band measurements, a digital predistorter has been extracted and tested.

The linearized amplifier complies the highly demanding WiMAX standard emission mask for modulating signal with PAPR of 9 dB.

In this condition, the linearized amplifier exhibits average efficiency of 40%, together with a gain of 10 dB, for an average power level of 34.2 dBm.

These performances place the present amplifier at the state of the art for this application.

ACKNOWLEDGMENTS

The authors wish to acknowledge the support of the Regione Piemonte NAMATECH project.

REFERENCES

[1] M. Steer, "Beyond 3G," *IEEE Microwave Magazine*, vol.8, no.1, pp.76-82, Feb. 2007, DOI 10.1109/MMW.2007.316254.

[2] S. Chia, T. Gill, L. Ibbetson, D. Lister, A. Pollard, R. Irmer, D. Almodovar, N. Holmes, S. Pike, "3G evolution," *IEEE Microwave Magazine*, vol.9, no.4, pp.52-63, Aug. 2008, DOI 10.1109/MMM.2008.924788.

[3] W.H., Doherty, "A New High Efficiency Power Amplifier for Modulated Waves," *Proceedings of the Institute of Radio Engineers*, vol.24, no.9, pp. 1163- 1182, Sept. 1936, DOI 10.1109/JRPROC.1936.228468.

[4] B. Kim, J. Kim, I. Kim, J. Cha, "The Doherty power amplifier," *IEEE Microwave Magazine*}, vol.7, no.5, pp.42-50, Oct. 2006, DOI 10.1109/MW-M.2006.247914.

[5] M. Iwamoto, A. Williams, Chen Pin-Fan, A.G. Metzger, L.E. Larson, P.M. Asbeck, "An extended Doherty amplifier with high efficiency over a wide power range," *Microwave Theory and Techniques, IEEE Transactions on*, vol.49, no.12, pp.2472-2479, Dec 2001, DOI 10.1109/22.971638.

[6] N. Srirattana, A. Raghavan, D. Heo, P.E. Allen, J. Laskar, "Analysis and design of a high-efficiency multistage Doherty power amplifier for wireless communications," *Microwave Theory and Techniques, IEEE Transactions on*, vol.53, no.3, pp. 852- 860, March 2005, DOI 10.1109/TMTT.2004.842505.

[7] Kyoung-Joon Cho, Jong-Heon Kim, S.P. Stapleton, "A highly efficient Doherty feedforward linear power amplifier for W-CDMA base-station applications," *Microwave Theory and Techniques, IEEE Transactions on*, vol.53, no.1, pp. 292- 300, Jan. 2005, DOI 10.1109/TMTT.2004.839341.

[8] J. Cha, J. Kim, B. Kim, J.S. Lee, S.H. Kim, "Highly efficient power amplifier for CDMA base stations using Doherty configuration," *Microwave Symposium Digest*, vol.2, pp. 533- 536 Vol.2, 6-11 June 2004, DOI 10.1109/MWSYM.2004.1336033.

[9] T. Yamasaki, Y. Kittaka, H. Minamide, K. Yamauchi, S. Miwa, S. Goto, M. Nakayama, M. Kono, N. Yoshida,"A 68 % Efficiency, C-Band 100 W GaN Power Amplifier for Space Applications," *Microwave Symposium Digest*, pp.1384-1387, 23-28 May 2010.

[10] K. Kuroda, R. Ishikawa, and K. Honjo, "Parasitic Compensation Design Technique for a C-Band GaN HEMT Class-F Amplifier," *Microwave Theory and Techniques, IEEE Transactions on*, vol.58, no.11, pp.2741-2750, Nov. 2010.

[11] J. Moon, J. Kim, I. Kim, Y.Y. Woo, S. Hong; H.S. Kim, J.S. Lee,B. Kim, "GaN HEMT Based Doherty Amplifier for 3.5-GHz WiMAX Applications," *Wireless Technologies, 2007 European Conference on*, pp.395-398, 8-10 Oct. 2007, DOI: 10.1109/ECWT.2007.4404030.

[12] Yong-Sub Lee, Mun-Woo Lee, Yoon-Ha Jeong, "Linearity Optimized 3.5 GHz GaN HEMT Doherty Amplifier," *The 23rd International Technical Conference on Circuits/Systems, Computers and Communications*, pp.1065-1068, July 6-9, 2008.

[13] J.-C. Park, D, Kim, Chan-Sei Yoo, W. Sung Lee, J.-G. Yook, C. K. Hahn, "Efficiency enhancement of the Doherty amplifier for 3.5 GHz WiMAX application using class-F circuitry," *Microwave and Optical Technology Letters*, Vol. 52, No. 3, pp. 570--573, March 2010, DOI 10.1002/mop.24977.

[14] P. Colantonio, F. Giannini, E. Limiti, "High Efficiency RF and Microwave Solid State Power Amplifiers," John Wiley & Sons, Ltd, 2009.

[15] J. M. Rubio, J. Fang, V. Camarchia, R. Quaglia, M. Pirola, G. Ghione, "3–3.6-GHz Wideband GaN Doherty Power Amplifier Exploiting Output Compensation Stages," *Ieee Transactions On Microwave Theory And Techniques* 60 (8), 2543-2548

[16] Jie Fang, R. Quaglia, J. Moreno Rubio, V. Camarchia,M. Pirola, S. Donati Guerrieri, G. Ghione, "Design and baseband predistortion of a 43.5 dBm GaN Doherty amplifier for 3.5 GHz WiMAX applications," *Microwave Integrated Circuits Conference, 2011. EuMIC 2011. European*, pp. 256-259, Manchester, 10 - 11 October 2011.

[17] J. Kim and K. Konstantinou, "Digital Predistortion of Wideband Signals Based on Power Amplifier Models with Memory," *Electron. Lett.*, vol. 37, pp.~1417-1418, 2001.

[18] J. Shealy, J. Smart, M. Poulton, R. Sadler, D. Grider, S. Gibb, B. Hosse, B. Sousa, D. Halchin, V. Steel, P. Garber, P. Wilkerson, B. Zaroff, J. Dick, T. Mercier, J. Bonaker, M. Hamilton, C. Greer, M. Isenhour, "Gallium nitride (GaN) HEMT's: progress and potential for commercial applications," *GaAs IC Symposium, 24th Annual Technical Digest*, pp. 243- 246, 2002.

[19] V. Camarchia, S. Donati Guerrieri, M. Pirola, V. Teppati, A. Ferrero, G. Ghione, M. Peroni, P. Romanini, C. Lanzieri, S. Lavanga, A. Serino, E. Limiti, L. Mariucci, "Fabrication and nonlinear characterization of GaN HEMTs on SiC and sapphire for high-power applications," International Journal of RF and Microwave Computer-Aided Engineering, Volume 16, Issue 1, pp. 70–80, January 2006.

[20] Cree, Inc., "CGH40010 Rev 3.1," Datasheet, {www.cree.com}.

[21] Jing Lu, Yan Wang, Long Ma, Zhiping Yu, "A new small-signal modeling and extraction method in AlGaN/GaN HEMTs," *Solid-State Electronics* Vol. 52 pp. 115--120, 2008.

[22] R. Quaglia, V. Camarchia, S. Donati Guerrieri, E. G. Lima, G. Ghione, Qiang Luo, M. Pirola, R. Tinivella, "Real-time FPGA-based baseband predistortion of W-CDMA 3GPP high-efficiency power amplifiers: comparing GaN HEMT and Si LDMOS predistorted PA performances," *Microwave Conference, 2009. EuMC 2009. European*, pp.342-345, Sept. 29 2009-Oct. 1 2009.

[23] M. Pirola, V. Teppati, V. Camarchia, "Microwave Measurements Part I: Linear Measurements," *IEEE Instrumentation and Measurement Magazine*, Vol. 10-2, pp. 14-19, 2007.

[24] V. Camarchia, V. Teppati, S. Corbellini, M. Pirola, "Microwave Measurements. Part II - Nonlinear Measurements," *IEEE Instrumentation and Measurement Magazine*, Vol. 10-3, pp. 34-39, 2007.

[25] T. Yamamoto T. Kitahara, S. Hiura, "50% Drain Efficiency Doherty Amplifier with Optimized Power Range for W-CDMA Signal," *Int. Microw. Symp. Dig.*, 2007, pp 1263 - 1266, DOI: 10.1109/MWSYM.2007.380422.

[26] V. Camarchia, F. Cappelluti, M. Pirola, S. Donati Guerrieri, G. Ghione, "Self-Consistent Electrothermal Modeling of Class A, AB, and B Power GaN HEMTs Under Modulated RF Excitation," *Microwave Theory and Techniques, IEEE Transactions on*, vol.55, no.9, pp.1824-1831, Sept. 2007, DOI: 10.1109/TMTT.2007.903839.

[27] ETSI EN 301 021, "Fixed Radio Systems; Point-to-multipoint equipment; Time Division Multiple Access (TDMA); Point-to-multipoint digital radio systems in frequency bands in the range 3 GHz to 11 GHz,".

[28] V. Camarchia, P. Colantonio, S. Donati Guerrieri, R. Giofre, E. G. Lima, M. Pirola, R. Quaglia, "Base-band Predistortion Linearization scheme of High Efficiency Power Amplifiers for wireless applications," *Proc. INMMiC 2008*, Malaga, Spain, November 2008.

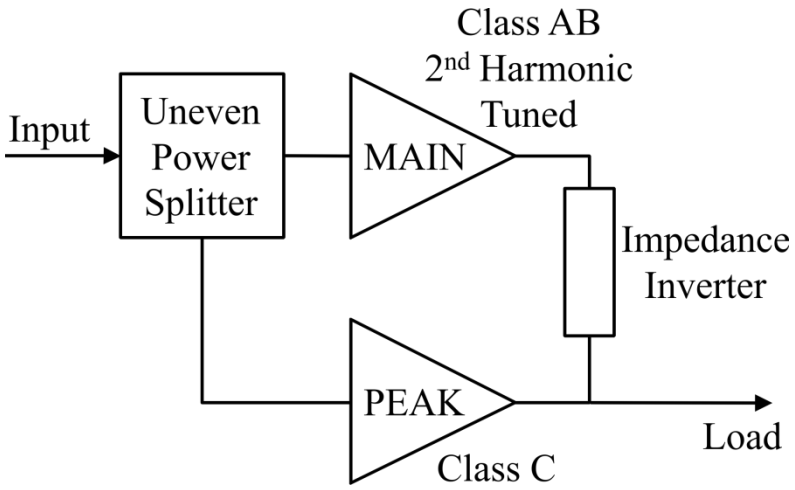

Fig. 13: Block diagram of the designed Doherty amplifier.

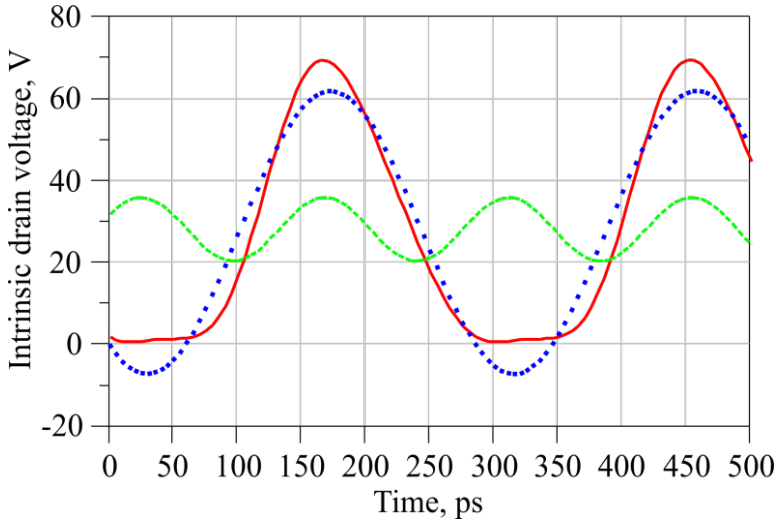

Fig. 14: Simulated drain voltage waveforms at 6 dB OBO (37.2 dBm): complete waveform (redline), fundamental (blue dotted line), and 2nd harmonic (green dashed line).

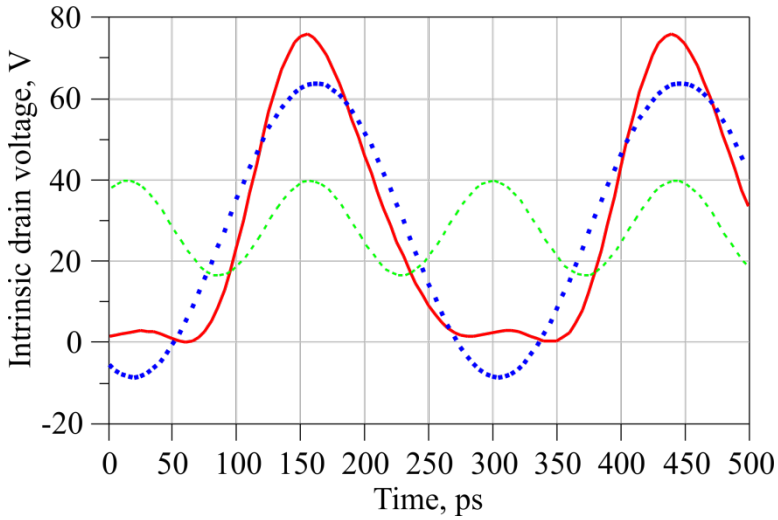

Fig. 15: Simulated drain voltage waveforms at saturated output power (43.2 dBm): complete waveform (red line), fundamental (blue dotted line), and 2nd harmonic (green dashed line).

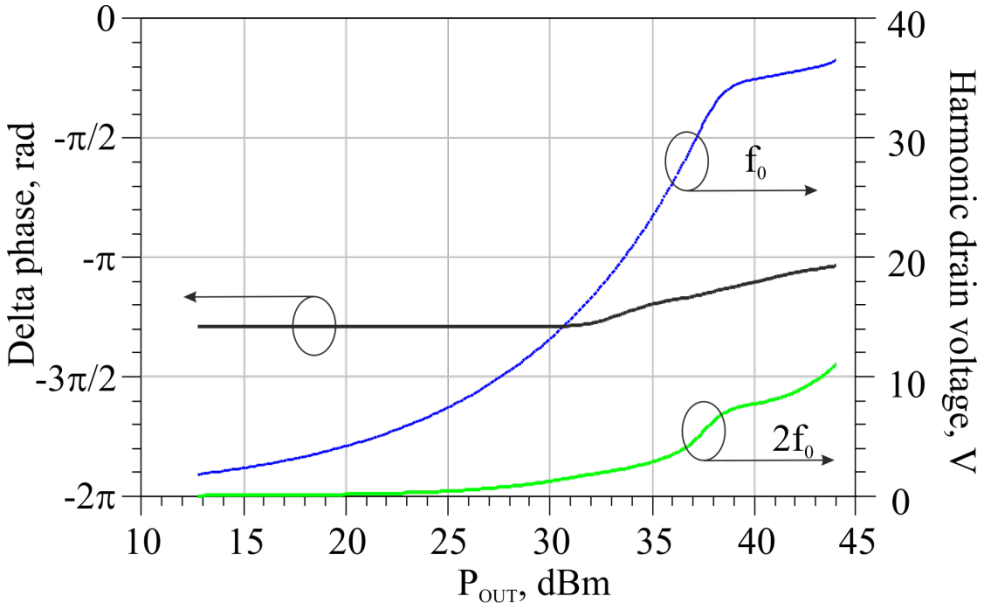

Fig. 16: Simulated amplitude of the fundamental (blue) and 2nd harmonic (green) of the main amplifier, together with their phase difference (black) versus output power.

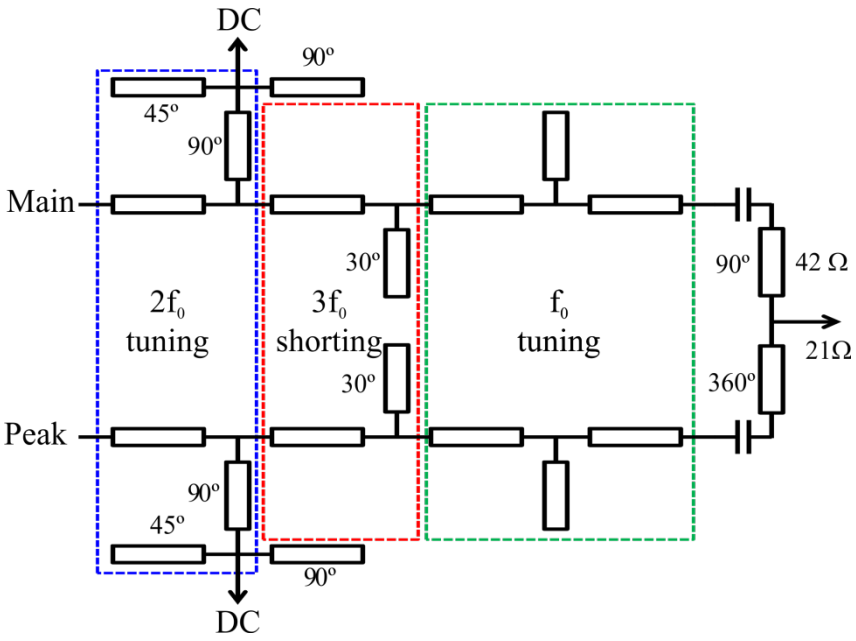

Fig. 17: Output matching network scheme of the Doherty PA.

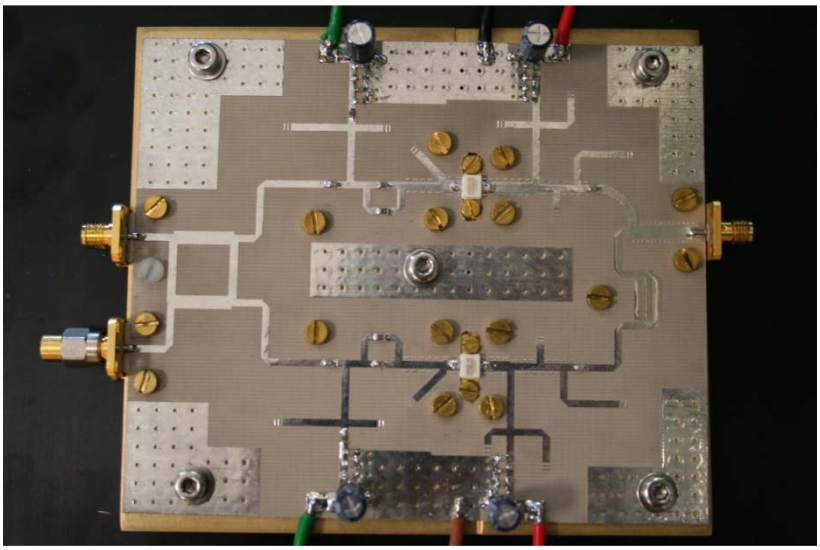

Fig. 18: Picture of the realized Doherty PA.

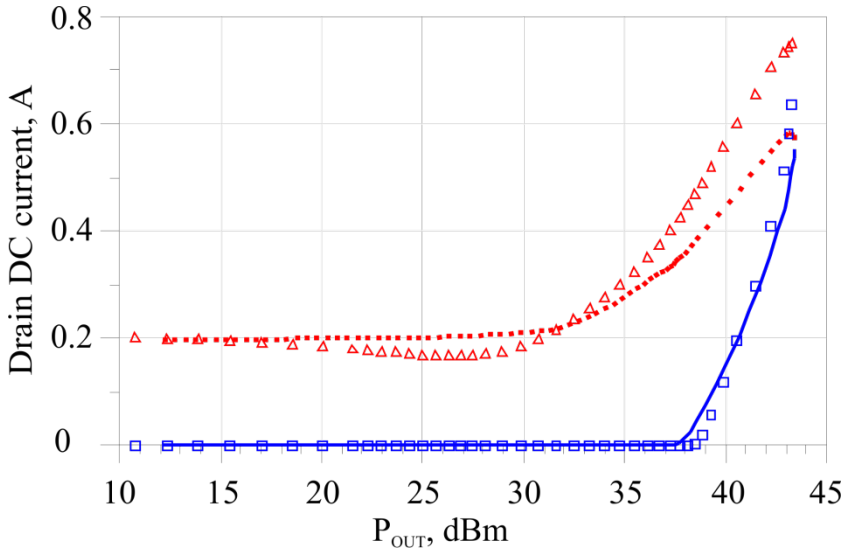

Fig.19: Main (red), and peak (blue) DC drain currents versus output power. Lines refer to simulations, while symbols to measurements.

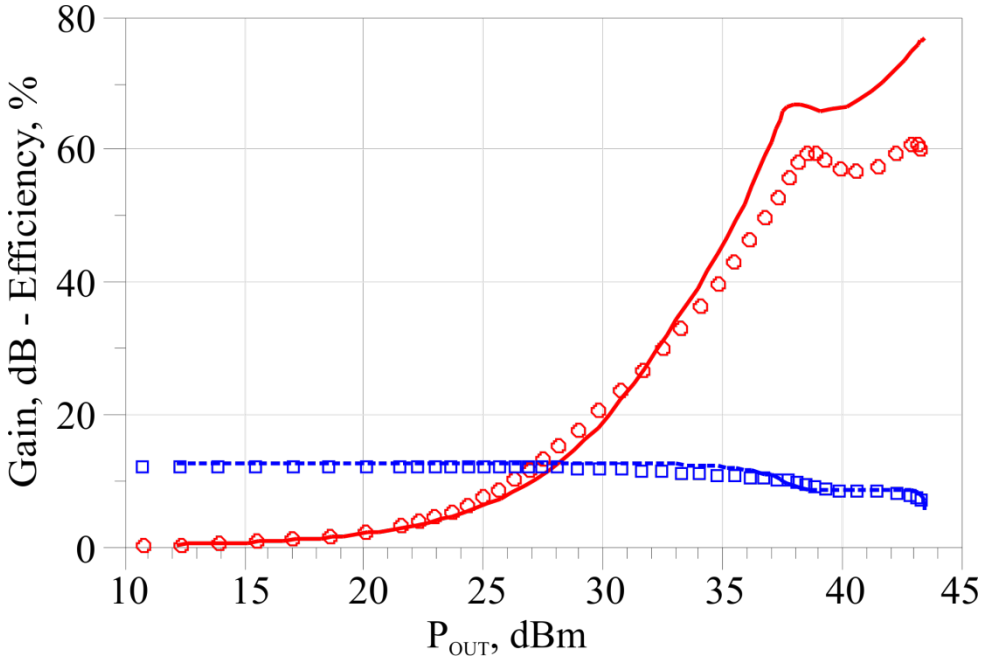

Fig. 20: 3.5 GHz, CW Single Tone PA characterization. Power Gain (blue), and Efficiency (red) versus output power. Lines refer to simulations, while symbols to measurements.

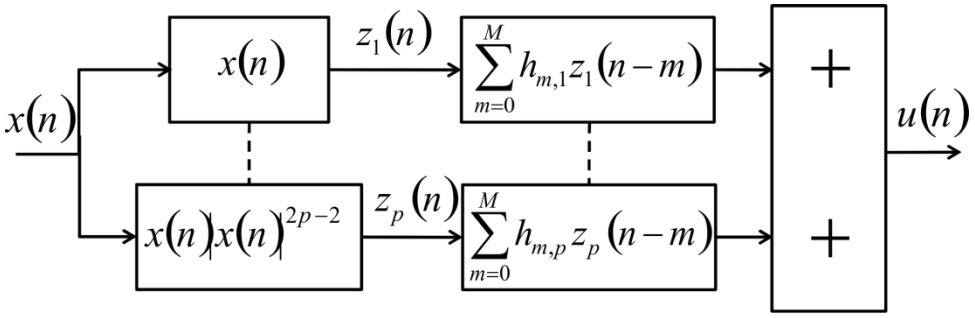

Fig. 21: Scheme of the Memory Polynomial base-band model.

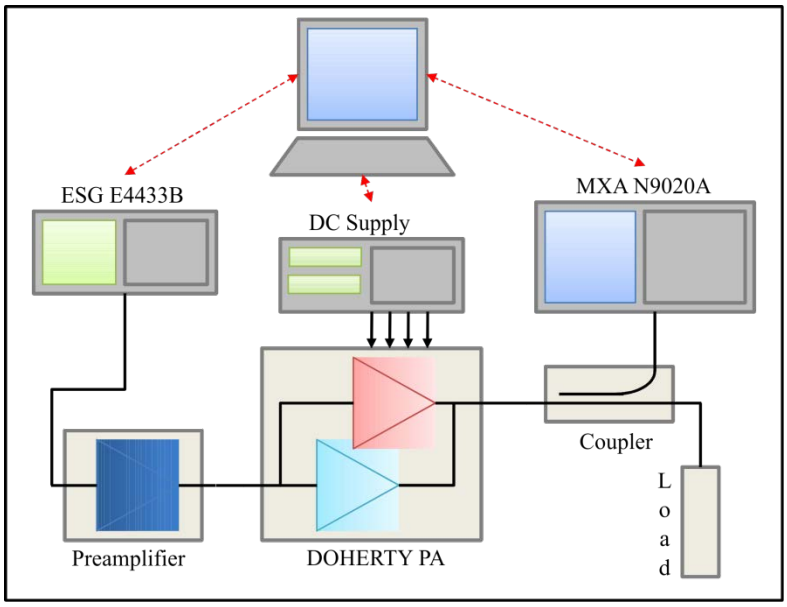

Fig. 22: Setup of the base-band characterization setup.

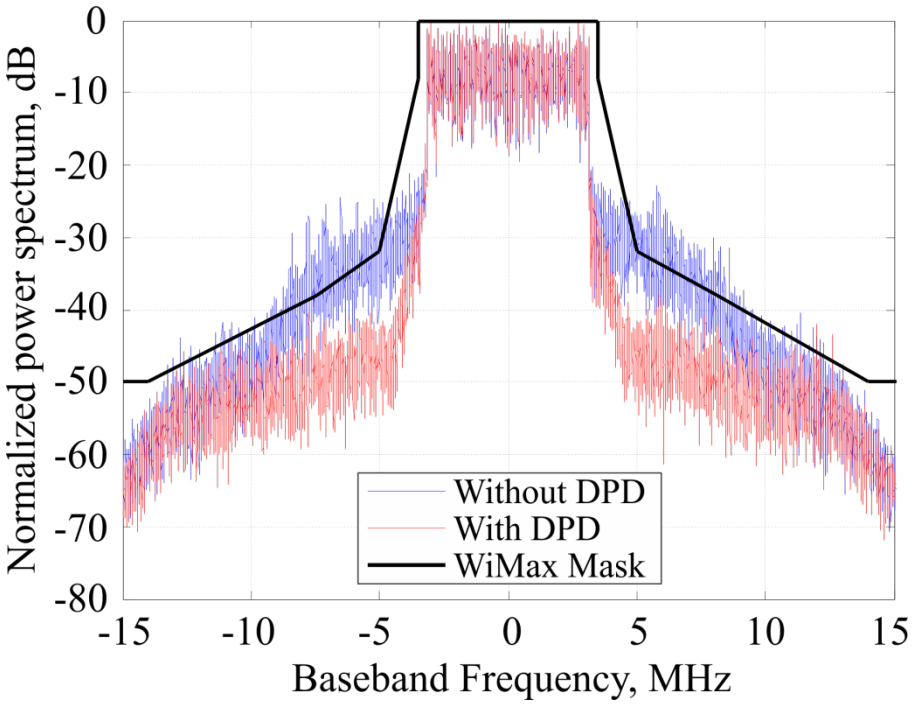

Fig. 23: Normalized output spectrum of the PA with (red) and without (blue) DPD, together with the WiMAX emission mask (black) [26].